

Orbit Newsletter Digital Publication

Q1 2022

Rub Diagnostics based on Vibration Data

Abstract

Vibration excursion in turbomachinery is troublesome, especially when approaching or exceeding a trip level. Understanding of its root-cause is extremely crucial for taking appropriate actions and resolving the issue. Rubs are certainly among the most common malfunctions that cause vibration excursion. This paper discusses how to diagnose rubs that typically occur in turbomachinery based on vibration data. These include rubs occurring in both steady-state and transient conditions. Selection and interpretation of vibration data plots such as trend, polar, Bode, orbit, and waterfall are illustrated that pinpoint rubbing and resulted shaft bow symptoms. All data presented have been obtained from real machines where rubs occurred. Mainly case studies are presented in this paper. The presented cases and concluded diagnostic rules using vibration data plots will help practicing engineers as well as enhance diagnostic tools.

Introduction

High vibration excursions in turbomachinery are often accompanied by malfunctions that need to be identified correctly. Such malfunctions, if not treated, may cause degradations in performance, unplanned shutdowns, or catastrophic failures. Rubs can often occur in turbomachinery, especially during the initial startup after an outage, or even for new units, due to tight seal clearance, changes in alignment condition, high unbalance response, etc. Distinguishing a rub from other malfunctions is extremely important for taking appropriate actions immediately, to avoid mechanical damage and ensure safe operations.

The topic of rub has been of great interest to many researchers in addition to practicing engineers. Taylor [1] and Newkirk [2] first reported and analyzed this behavior. In turbomachinery, stationary components such as packings, seals, and oil deflectors are used to separate two fluids around the rotor. When the rotor contacts the stationary elements, heat is generated to deform the rotor thermally, thus creating equivalent unbalance in addition to frictional force due to rubbing to cause changes predominantly in 1X synchronous vibration. This thermal rub behavior is now known as the Newkirk effect. Since these days rotors have become longer and more flexible with tighter clearance, the rubbing issue can be more pronounced.

Besides the Newkirk effect, full annular rub was studied by many researchers. This includes forward precessional full annular rub with 1X synchronous vibration when passing a resonant speed, as well as reverse precessional full annular rub, often called dry whirl or whip with frequency close to the lowest natural frequency. These studies can be found from works by Black [3, 4], Crandall and Lingener [5, 6], Muszynska [7], Yu [8, 9], and Childs [10, 11]. These cases, however, have hardly occurred in real machines besides those in experimental setups. Moreover, bouncing type of rub with fractional frequency of the running speed, often called normal-tight, was studied by Bently [12]. Though this type of rub can be easily generated with the $\frac{1}{2}X$ vibration in a rotor kit with a brass screw, it does not occur very often in real machines either. Instead, the $\frac{1}{2}X$ vibration in real machines usually indicates normal-loose cases such as an oversize bearing or bearing looseness as reported by Yu [13].

From cases in real machines as directly experienced and reviewed by the author for the past decade, almost all the rub cases were accompanied by 1X vibration excursions as a result of the Newkirk effect. Many analytical and experimental studies besides Newkirk and Taylor have been performed, such as those by Dimarogonas [14], Muszynska [15], and Sawicki [16]. There are many other root-causes that can also lead to 1X vibration excursions besides rubs, such as thermal transient and peak conditions, generator thermal sensitivity, steam loading, changes in alignment condition, the Morton effect [17], etc. Current available vibration data collection and monitoring systems can yield various vibration data plots besides readings. How to select and interpret vibration data plots that are related to rubs is imperative to resolve machinery and vibration issues correctly and quickly. This paper presents rub cases from real machines to show how rubs can be effectively diagnosed based on vibration data.

Case study 1

This case occurred on a steam turbine generator with power output of approximately 9 MW. The double-flow steam turbine with rated speed of about 4350 rpm drove the 1800 rpm 4-pole generator via a speed reduction gearbox. Its machine train diagram is shown in Fig. 1. When viewed from the turbine towards the generator, the turbine is seen to be rotating in the clockwise direction. Vibration on the turbine is monitored by proximity probes only in the vertical direction at both inboard (IB) and outboard (OB) bearings.

High vibration excursions occurred on the steam turbine rotor, and consistently tripped the unit during startup or at rated speed. Therefore, the author was requested to diagnose the root-cause of the high vibration. An optical Keyphasor® probe was temporarily installed to measure once-per-turn signals for obtaining filtered 1X vibration data. Independently-wired velocity transducers were also mounted temporarily to verify if vibration excursions from proximity probes were real. All these signals along with those from existing proximity probes were wired to Bently Nevada®ADRE data acquisition system.

Fig. 2 shows direct and 1X-filtered vibration trend plots measured by two proximity probes in the top vertical direction at both IB and OB bearings of the turbine along with speed trend. Trend plots present general information regarding levels of vibration, and typically are used for the purpose of monitoring. At rated speed of around 4350 rpm, direct vibration amplitude at IB bearing kept increasing. After 20 minutes, it increased from approximately 1 mil pp to 4 mil pp. If only the direct amplitudes are plotted, it would be very difficult to diagnose the problem. However, since the 1X amplitudes are included, one can see that the vibration excursion was predominantly composed of the 1X component. Unfortunately, majority of turbomachinery vibration issues are due to the 1X vibration and many malfunctions could yield high 1X vibration excursion.

To help diagnose the problem, other types of vibration plots should be used. Bode plots can be used effectively to see vibration versus speed. Fig. 3 shows 1X Bode plots measured by the two proximity probes. Three different colors are used to distinguish among startup (blue color), steady-state or rated speed (red color), and shutdown (green color) conditions. As one can see, the 1X vibration started low at both OB and IB bearings. The unit then reached a heat-soak speed of around 1800 rpm.

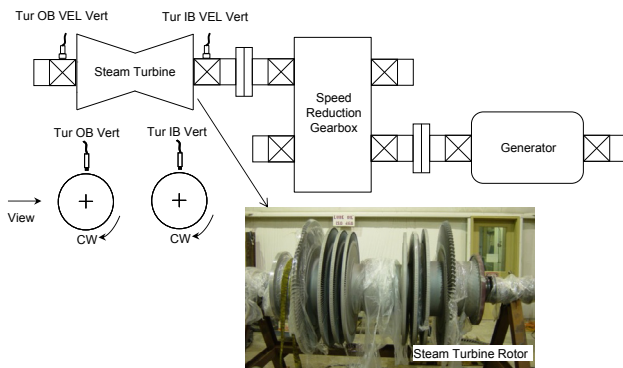


Figure 1: Machine train diagram for Case 1

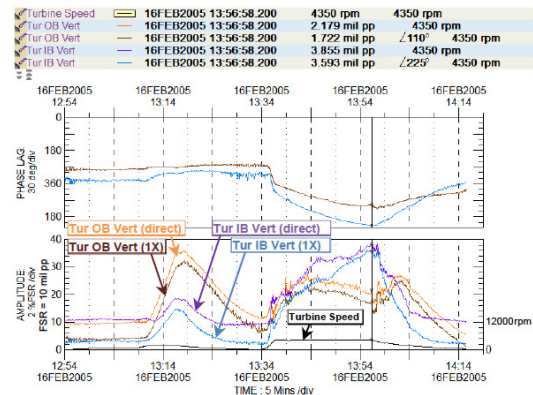


Figure 2: Direct and 1X vibration trend plots measured by proximity probes at turbine OB and IB bearings along with speed

5 minutes after staying at this constant speed, however, the 1X vibration at both OB and IB bearings increased dramatically. The 1X amplitude at OB bearing had a rise from 0.5 mil pp to 3 mil pp. The unit was then brought down to below 200 rpm. As indicated in the Bode plot, the 1X amplitudes were much higher throughout the speed range from 200 rpm to 1800 rpm during coast-down than during startup. This indicates thermal bow due to rubbing developed and reduced to some degree when speed reduced to around 200 rpm. The unit was then brought up again to rated speed of 4350 rpm. Note that the 1X amplitudes during the re-startup already became higher than during the initial startup for the same speed in the speed range from 200 rpm to 1800 rpm due to residual shaft bow. At rated speed of 4350 rpm, vibration kept increasing. 20 Minutes after staying at 4350 rpm, the 1X vibration at IB bearing increased from 0.8 mil pp to 3.6 mil pp. Changes in 1X vibration at this

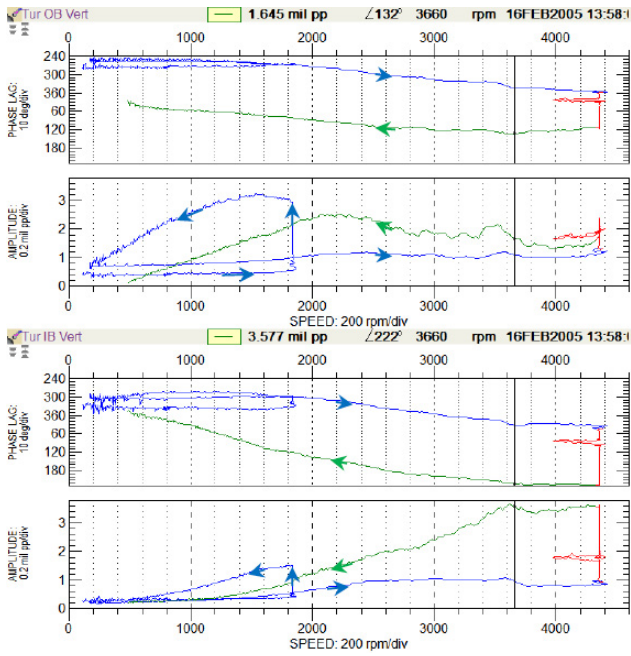


Figure 3: IX Bode plots measured by proximity probes at turbine OB and IB bearings

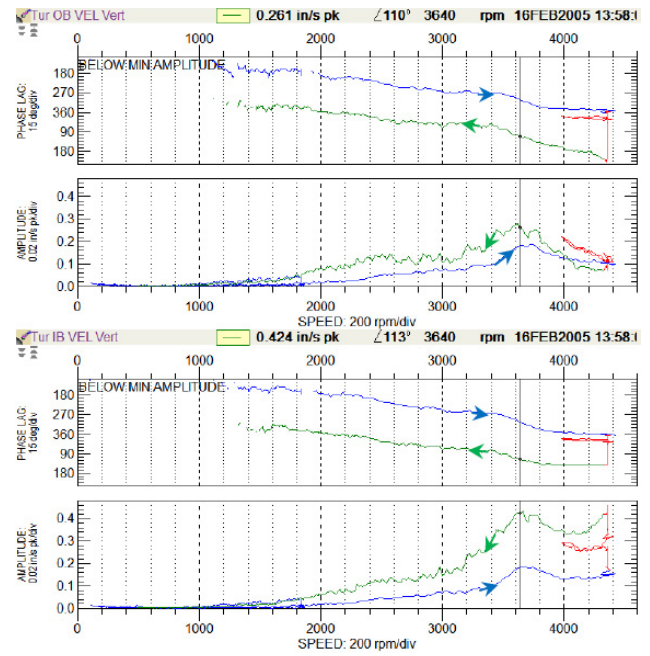


Figure 4: IX Bode plots measured by velocity transducers at turbine OB and IB bearing caps

constant rated speed cannot be fully presented from Bode plots. Due to the high vibration excursion that kept increasing its level, the unit was shut down. The IX amplitudes were significantly higher during shutdown than during startup due to developed thermal bow from rubbing. Bode plots from proximity probes can show not only high vibration due to shaft bow from rubbing, but also shaft bow directly at low speed. Fig. 4 shows IX Bode plots measured by two velocity transducers mounted on bearing caps parallel to the existing proximity probes. Unlike the proximity probes, these two velocity transducers could not clearly capture rub behavior at the heat-soak speed of around 1800 rpm as well as shaft bow below that speed from the Bode plots. Higher amplitudes at speed range above 1800 rpm during shutdown than during startup were observed along with casing resonance of around 3600 rpm. IX peak amplitudes, however, appeared to capture the casing resonance of around 3640 rpm, as marked by the cursor in the plots, during both startup and shutdown conditions.

Figs. 5 and 6 show polar plots measured by proximity probes and velocity transducers, respectively. It would be difficult to diagnose if a rub exist during transient startup or shutdown condition where speed varies from polar plots. However, when speed is constant during steady-state condition, IX vectors tend to remain almost constant as well for a machine without any issues. The red color in Figs. 5 and 6 designates steady-state condition at rated speed of 4350 rpm. Within 20 minutes at this speed, IX vectors from both proximity probes and velocity transducers kept rolling in the direction against the shaft rotation. Higher level vibration excursion occurred at inboard than at outboard. The IX vector at inboard bearing changed from approximately 1 mil pp to 3.5 mil pp measured by the proximity probe, and from 0.15 in/s pk to 0.45 in/s pk measured by the velocity transducer within the 20 minutes. From the trending of polar plots, had the machine kept running at this rated speed, vibration would have kept increasing. Polar plots at constant rated speed from either proximity probes or casing-mounted velocity transducers can effectively pinpoint the Newkirk effect due to rubbing.

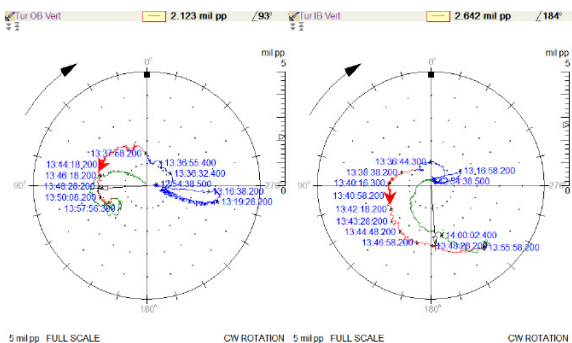


Figure 5: IX polar plots measured by proximity probes at turbine OB and IB bearings

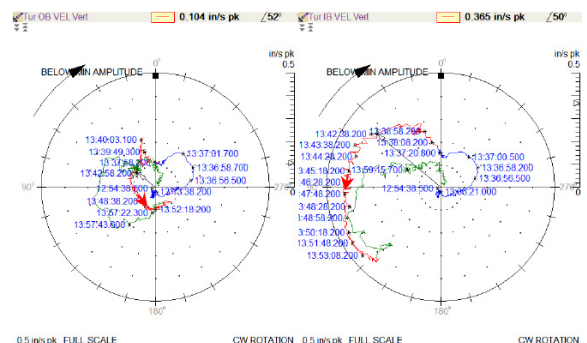


Figure 6: IX polar plots measured by velocity transducers at turbine OB and IB bearing caps

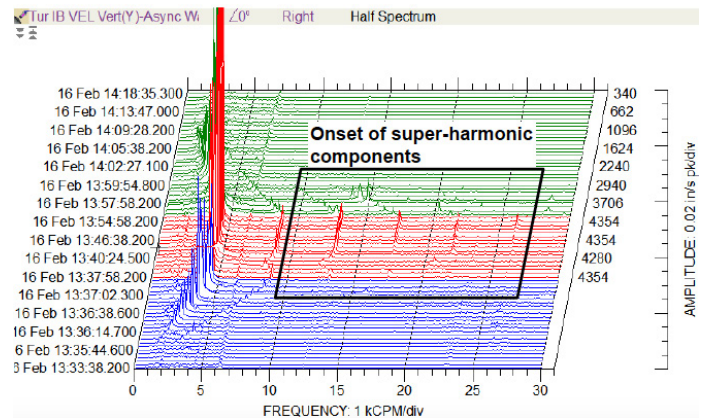
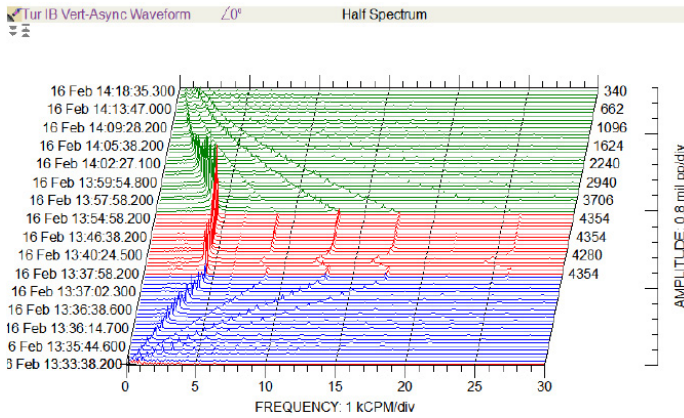
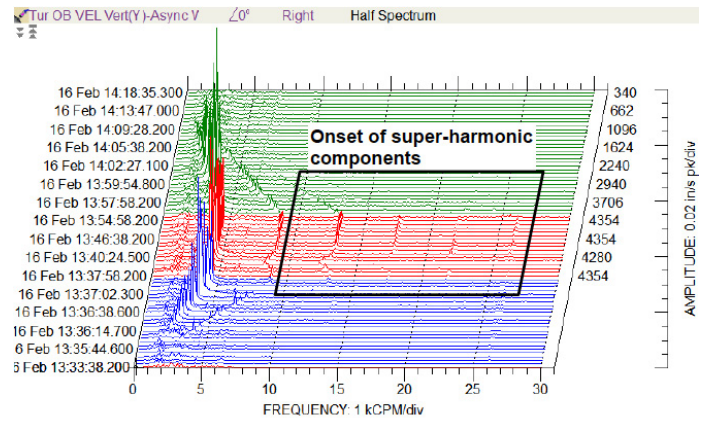
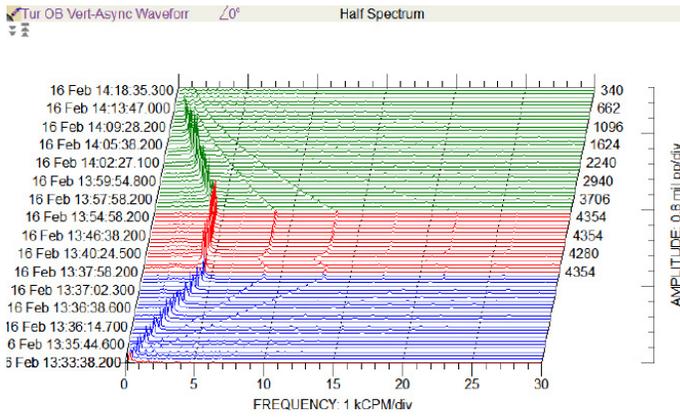


Figure 7: Waterfall plots measured by proximity probes at turbine OB and IB bearings

Figure 8: Waterfall plots measured by velocity transducers at turbine OB and IB bearing caps

Figs. 7 and 8 show waterfall plots measured by proximity probes and velocity transducers, respectively. It appears that super-harmonic components such as 2X, 3X and 4X from proximity probes existed at all times (see Fig. 7). Mechanical and electrical runout on the probe-viewing area could contribute to these components. However, 3X to 6X components from velocity transducers only presented when rubbing occurred (See Fig.8). These components resulted from high non-linear vibration response due to rubbing contact. Onset of rich super-harmonics from casing-mounted transducers appears to be a symptom of rubbing contact.



Figure 9: Signs of rub as seen from turbine rotor and top case

Case study 2

This case involves a steam turbine generator with power output of approximately 28 MW. An 1800 rpm 4-pole water-cooled generator was driven by a 3000 rpm steam turbine via a speed reduction gearbox. Its machine train diagram is shown in Fig. 10. When viewed from the turbine towards the generator, the generator is seen to be rotating in the counter-clockwise direction. Vibration is monitored by a pair of X-Y proximity probes at each bearing.

High vibration occurred from generator bearings during startup as well as at rated speed of around 1800 rpm. Due to high vibration readings, the machine was shut down 30 seconds after attaining full-speed-no-load (FSNL) condition.

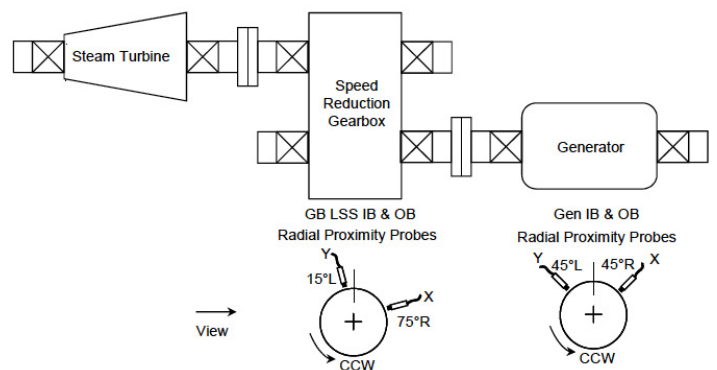


Figure 10: Machine train diagram for Case 2

Vibration was predominantly composed of the 1X component. No vibration excursion was observed from either turbine or gearbox high speed shaft bearings.

Fig. 11 shows 1X Bode plots measured by proximity probes in the X-direction at generator and gearbox low speed shaft bearings. Since vibration was higher in the X-direction than in the Y-direction in this case for the counter-clockwise rotating generator rotor and gearbox low speed shaft (horizontal and gravity loaded), vibration levels in the X-direction were used in these Bode plots. Three different colors are used to distinguish among startup (blue color), FSNL (red color), and shutdown (green color) conditions. During startup up to 1500 rpm, vibration remained low at all bearings. Even at the first critical speed of around 1200 rpm, peak amplitudes were still below 1.5 mil pp. However, when speed increased from 1500 rpm to 1800 rpm, vibration at generator inboard bearing increased to approximately 5 mil pp. The machine was then shut down approximately 30 seconds after staying at FSNL condition. During shutdown, vibration still kept increasing even after passing the first critical speed of around 1200 rpm. At 1000 rpm, vibration at generator inboard bearing reached over 8 mil pp. The Bode plots indicate shaft thermal bow due to a rub on the generator rotor. Vibration at gearbox low speed shaft bearings was also affected due to the generator rotor bow.

Fig. 12 shows orbits from generator outboard bearing to low speed shaft outboard bearing (in order from top to bottom) at three different times (in order from left to right). These orbits are waveform-compensated by samples at 190 rpm to get rid of probe-viewing area runout effects. The Bode plots in Fig. 11 pinpoint that a rub likely started when speed increased from 1500 rpm during startup. Examining all the four orbit plots at 1822 rpm, one can see clearly a distorted orbit from the generator inboard bearing due to a hard rub. Orbit from the generator inboard bearing, though flat, could occur sometimes due to bearing loading issues. Orbits from gearbox low speed shaft bearings do not present symptoms of malfunction. During shutdown, rubbing maintained until speed below 1000 rpm. Similar orbits at 1150 rpm can be observed with even more distorted shape from the generator inboard bearing, indicating that rubbing was still engaged at that speed. At speed of 540 rpm, orbit from the generator inboard bearing became normal and smooth without any restricted shape or abrupt change, indicating that rubbing was most likely disengaged though amplitude was still around 5 mil pp. The reason that the amplitude still remained high was because the thermal bow due to rubbing still remained. In short, the distorted orbit with abrupt change from the generator inboard bearing while orbits from other bearings appear normal indicates that the rubbing occurred

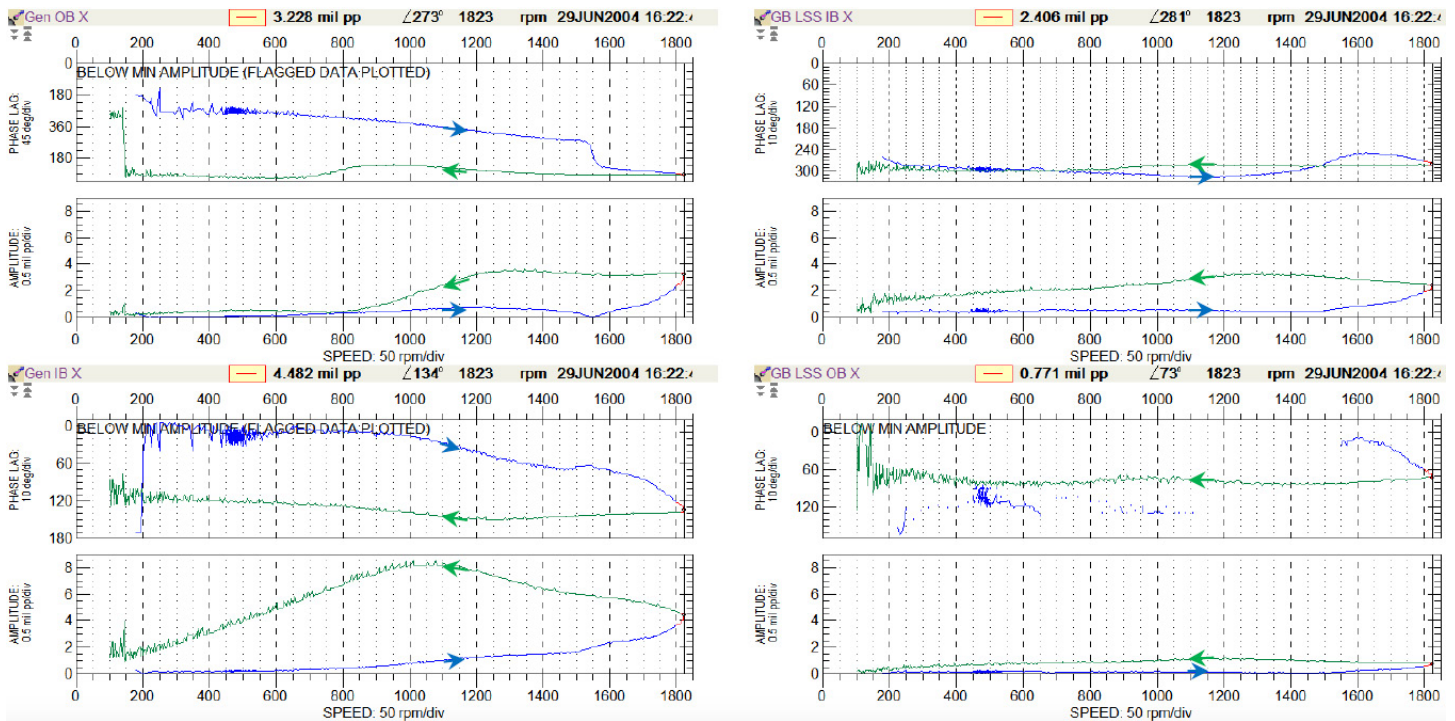


Figure 11: 1X Bode plots measured by proximity X probes at generator bearings (left) and gearbox low speed shaft bearings(right)

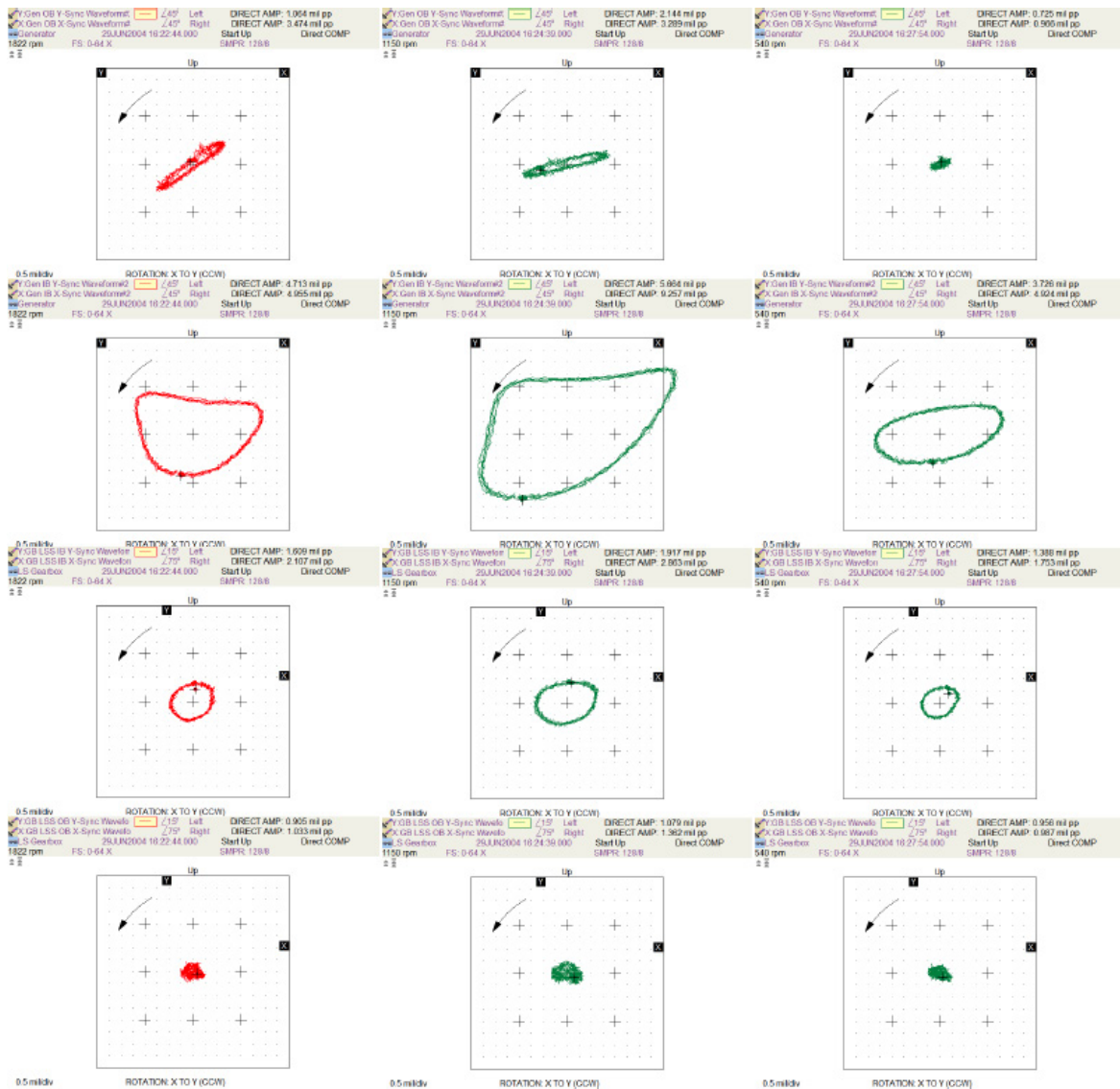


Figure 12: Waveform-compensated orbits at generator and gearbox low speed shaft bearings as rub occurred (1822 rpm on the left and 1150 rpm in the middle) and then disengaged (540 rpm on the right)

near the generator inboard bearing, possibly against the oil deflector for this water-cooled generator. Changes in orbit shape help to determine rubbing location and duration.

Fig. 13 shows a full-spectrum waterfall plot measured by a pair of X and Y probes at the generator inboard bearing. Super-harmonic components presented when this hard rub occurred. Forward 4X and 5X components, accompanied by reverse 3X and 4X components, appeared when rubbing occurred. This can be explained by the observed abnormal orbit shape, which corresponds to rich super-harmonic components when FFT was performed on these irregular waveforms in time base.

Note that trend and polar plots are not presented here due to lack of enough constant-speed data at FSNL condition. The unit started up and then shut down immediately from FSNL condition. When speed varies, examining trend or polar plots would not yield additional convincing information for rub detection because 1X vibration is supposed to change with speed even in normal condition.

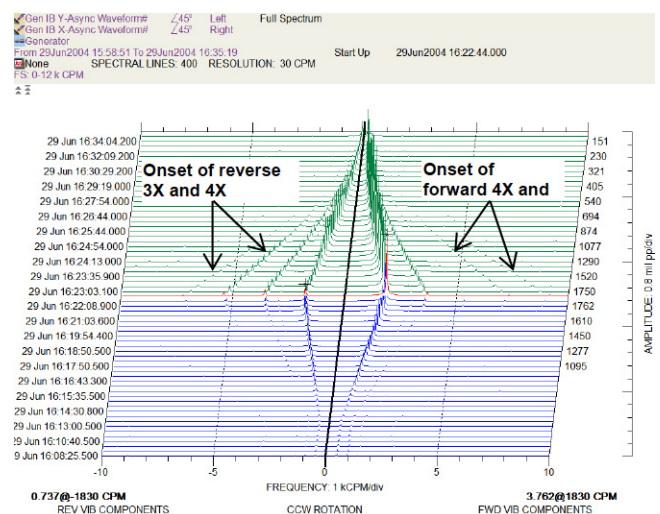


Figure 13: Full-spectrum waterfall plots measured by a pair of X and Y proximity probes at generator IB bearing

Case study 3

In the third case, multiple rubs occurred on a steam turbine generator unit with power output of approximately 180 MW. The steam turbine is made up of HP (high pressure)-IP (intermediate pressure) and LP (low pressure) rotors, driving a 3600-rpm generator. Its machine train diagram is shown in Fig. 14. Shaft rotation direction is considered to be counter-clockwise when viewed from driver to driven. Both the steam turbine and the generator vibrations are measured by X-Y pairs of non-contacting proximity probes mounted at 45-degree left (Y-probe) and 45-degree right (X-probe) relative to the 0 degree vertical reference at each bearing from Bearing # 1 to #6, which are named as Bearing T1 to T6.

For this unit being horizontal and gravity loaded with counter-clockwise rotation, vibration readings are typically higher from probes mounted at 45-degree right (X-probe) than from those at 45-degree left (Y-probe). Therefore, when trend or polar plots are presented, vibration variables only from X-probes are selected.

During the initial run up to 15 MW after an outage, variation of vibration readings, almost totally composed of the 1X component, was observed mainly at T5X (Bearing #5 X-probe) and T6X (Bearing #6 X-probe). The variation was also observed at T3X (Bearing # 3 X-probe) and T4X (Bearing #4 X-probe) to a lesser extent. Fig. 15 shows 1X trend plots from T3X to T6X at rated speed of 3600 rpm. 1X amplitudes at T5X and T6X varied from 0.5 mil pp to 3 mil pp along with changes in phase angles during the run.

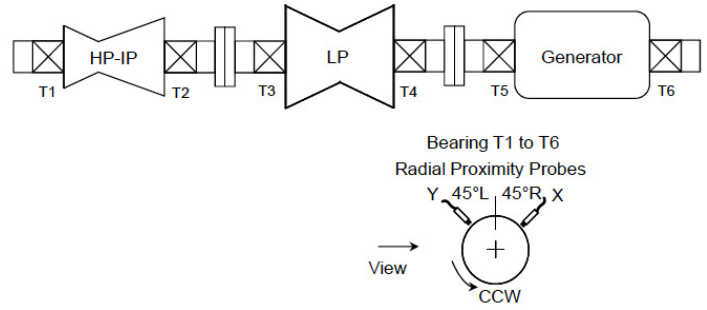


Figure 14: Machine train diagram for Case 3

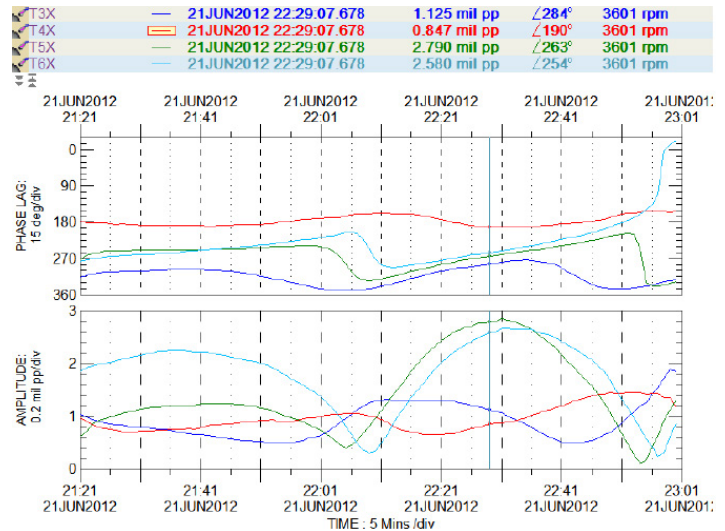


Figure 15: 1X vibration trend plots measured by T3X to T6X at rated speed of 3600 rpm with power output up to 15 MW at turbine OB and IB bearing caps

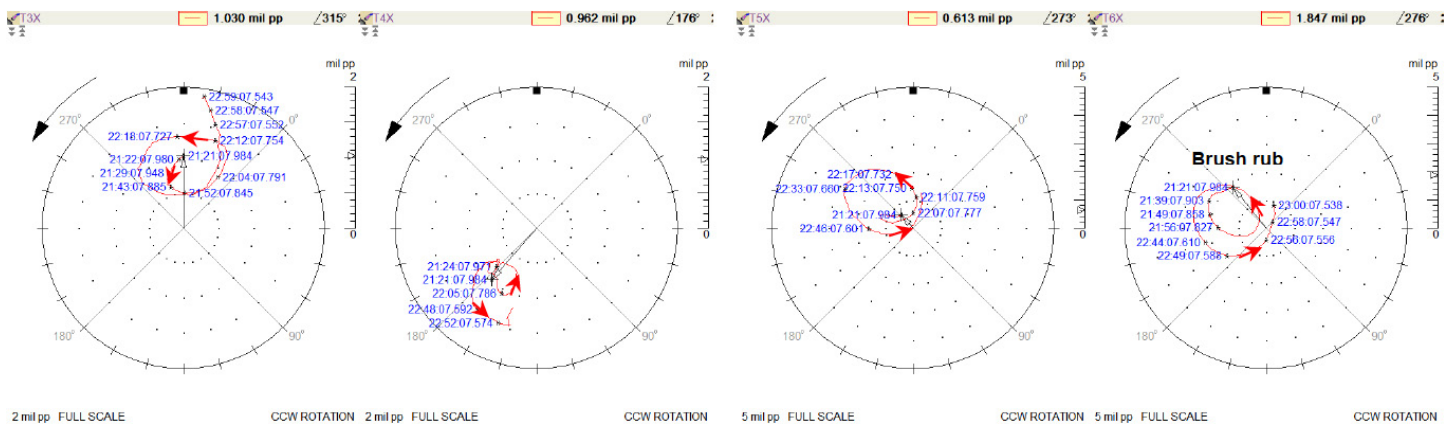


Figure 16: 1X polar plots measured by T3X to T6X at rated speed of 3600 rpm with power output up to 15 MW

1X polar plots from T3X to T6X indicate that the 1X vectors were rolling in the same direction as shaft speed, as shown in Fig. 16. This pinpoints a light rub against grounding carbon brush rings located between T4 and T5, as seen from similar units. It is usually caused by uneven or non-concentric contact between the rotor and the brush rings. A further test can be done by lifting one out of four brush rings to see whether 1X vibration changes or not for verification. Once the carbon brushes are replaced with the copper wire braid, oscillation of amplitudes will disappear. As expected, this brush-type rub behaved as a limit cycle with vibration not exceeding 3 to 4 mils pp at T5X and T6X, and also affected turbine bearing vibration readings to a lesser extent.

During the second run up to 63 MW, however, the unit tripped when direct vibration at T6X reached over 9 mil pp. Fig. 17 shows 1X trend plots measured from T3X to T6X. When 1X vibration reached close to 9 mil pp at T6X, 1X amplitude at T3X also reached over 6 mil pp. Examining polar plots as shown in Fig. 18 indicates that 1X vectors changed their pattern from rolling in the same direction as shaft speed due to brush rub, to moving radially outward or slightly rolling opposite to the

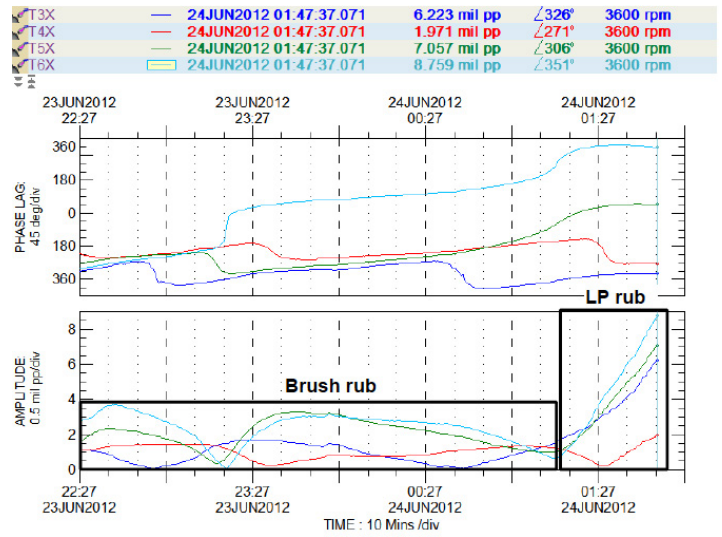


Figure 17: 1X vibration trend plots measured by T3X to T6X at rated speed of 3600 rpm with power output up to 63 MW (unit tripped due to direct amplitude over 9 mil pp at T6X)

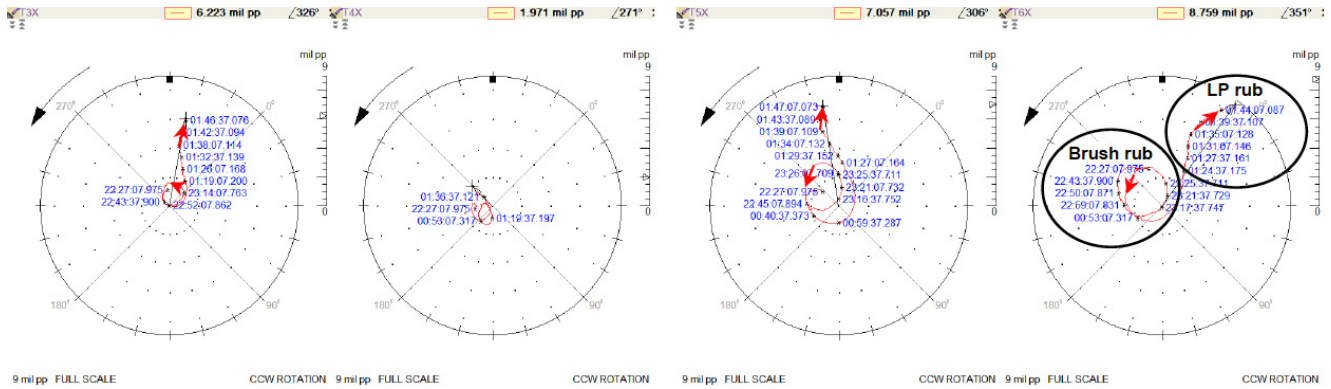


Figure 18: 1X polar plots measured by T3X to T6X at rated speed of 3600 rpm with power output up to 63 MW (unit tripped due to direct amplitude over 9 mil pp at T6X)

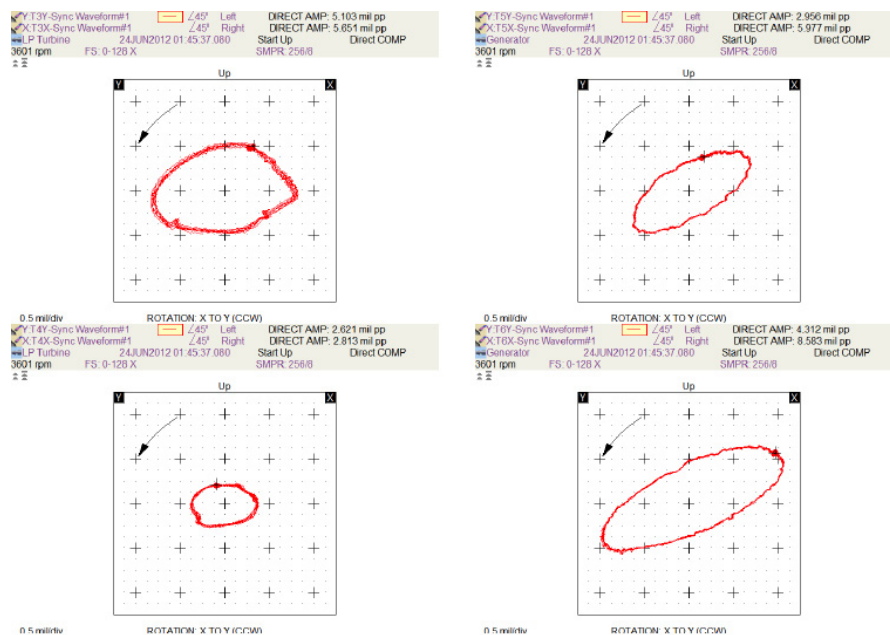


Figure 19: Waveform compensated orbits from T3 to T6 when vibration excursion approached trip level at 63 MW

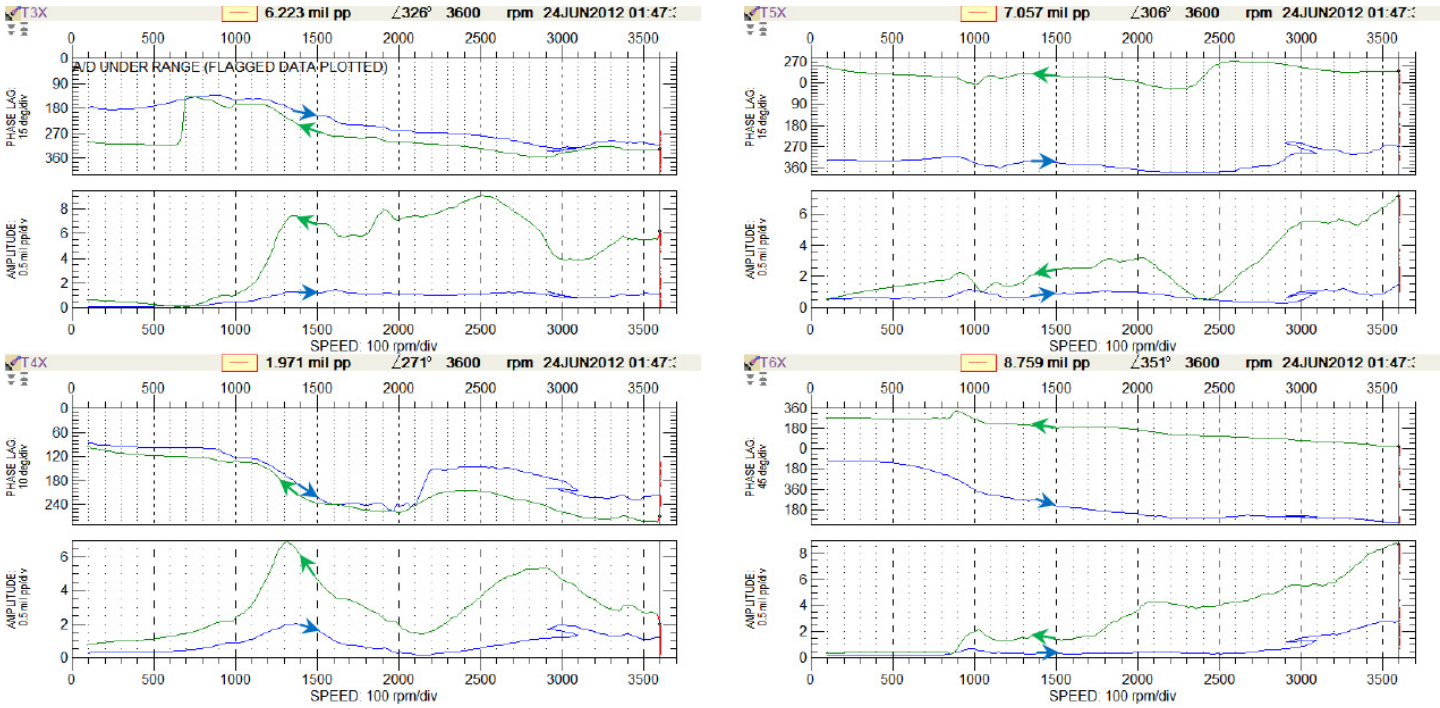


Figure 20: 1X Bode plots measured by T3X to T6X during startup, and shutdown due to high vibration trip at 63 MW

shaft speed direction. This indicates that a seal or packing rub on the LP rotor occurred during the time when the brush-type rub still maintained. Since the generator rotor ran close to the third mode, thermal bow from the adjacent LP rotor would affect vibrations at generator bearings more dramatically than at LP bearings.

Fig. 19 shows waveform-compensated orbits from T3 to T6 when direct vibration readings reached over 6 and 8 mil pp at T3X and T6X respectively. Distorted orbits can be seen on the LP bearings, especially at T3. 1X Bode plots measured by T3X to T6X, as shown in Fig. 20, clearly indicate significant difference between startup and shutdown conditions. It appears that the LP shaft bow due to rubbing caused high peak response especially near its first critical speed of about 1300 rpm. The generator rotor, however, did not experience high peak response near its first critical speed of about 1000 rpm.

During the following run up to 85 MW, several vibration excursions occurred but did not trip the unit, as shown in Fig. 21. The first vibration excursion was caused by a

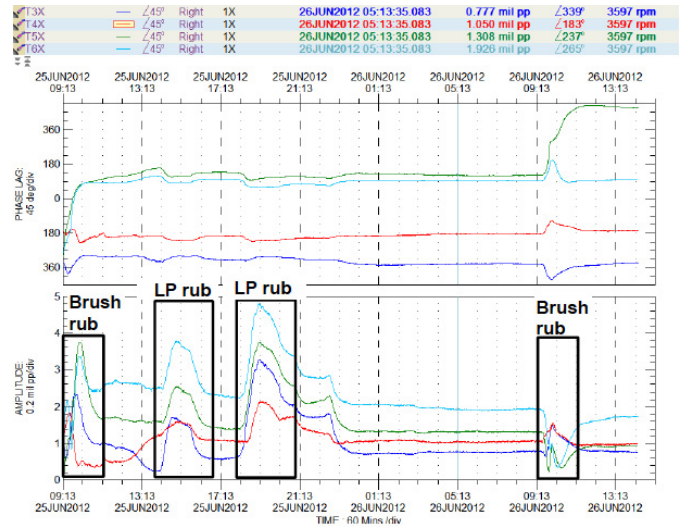


Figure 21: 1X vibration trend plots measured by T3X to T6X with multiple vibration excursions at 85 MW

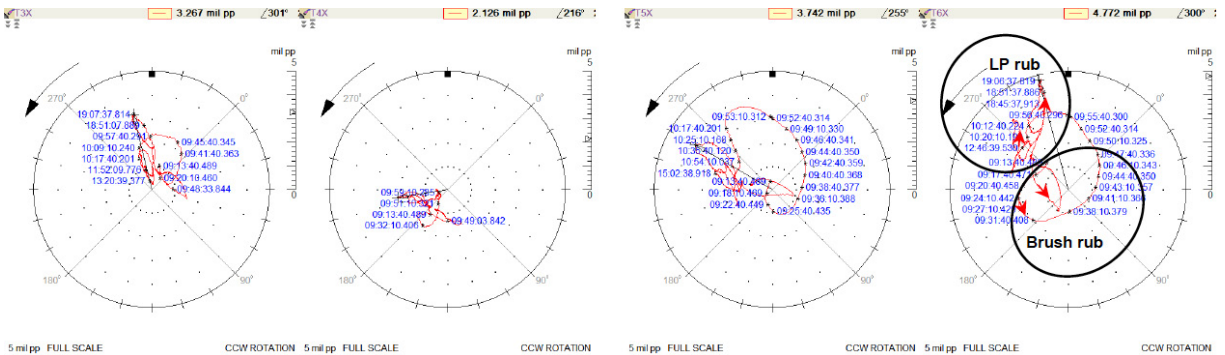


Figure 22: 1X polar plots measured by T3X to T6X with multiple vibration excursions at 85 MW

brush-type rub based on forward rolling 1X vectors in polar plots as shown in Fig. 22. Vibration due to the brush-type rub typically would not exceed to the trip level. The second and third vibration excursions were triggered by hot reheat or LP bypass valve opening events. Some of spray nozzles were likely plugged so that uneven steam spray within the condenser might have caused uneven thermal distortion on the LP turbine casing. As a result, the LP rotor touched packing or seal. The resulting high 1X vectors from rubs due to bypass valve opening events were different from previously observed rubs. This indicates more than one location of rubbing on the LP rotor. When vibration excursions occurred that was not due to the brush rub, slightly reducing MW alleviated rub condition and avoided a vibration rise to the trip level. A week later, the unit was successfully brought to base load condition with low vibration readings.

Summary and Discussion

Rubs are typically associated with high 1X vibration excursions as a result of the Newkirk effect. There are, of course, many other factors including thermal transient conditions, generator thermal sensitivity, steam loading, changes in alignment condition, and the Morton effect can also be related to changes in 1X vibration. Therefore, a comprehensive review of vibration data is needed to ensure correct diagnostics. Due to the page limit, the current paper only demonstrates three cases of rub. From numerous rub case histories including these three, it is shown that selection of proper data plots and capture of key features are crucial to the success of rub diagnostics. Table 1 lists these relevant plots and their features related to rubs.

Vibration data formats that can be used to diagnose rubs include trend, polar, Bode, orbit, and waterfall plots, as shown in Table 1. X-Y orthogonally mounted proximity probes are preferred to casing-mounted velocity transducer for rub diagnostics for machines supported by fluid film bearings. The former can generate orbits and show shaft bow even at low speed, though the latter can yield waterfall plots to show true super-harmonics if any.

Trend plots, used to detect changes of any measured variable from any data channel over a period of time, can be employed to observe whether 1X vibration amplitudes and phase angles vary with time or not. These plots should contain 1X vibration and be reviewed for data range during steady-state or almost constant speed condition. Readings from proximity probes or casing-mounted transducers should remain almost constant or stabilized with time if no rub or other malfunctions occur. Review of other data plots is often needed to assist rub diagnostics. Looking into 1X phase angles from trend plots only may sometimes yield a skewed impression of how 1X vectors vary including the direction and extent of rolling.

Polar plots, used to display filtered amplitude and phase angle as a function of speed or time in polar co-ordinates, can be best employed to see how 1X vectors change with time. Data review should be focused on steady-state or almost constant speed condition. If no rub or other malfunctions occur at constant speed, the data points would not move. For most rubs, 1X vectors would roll in the opposite direction to the shaft speed or move radially outward. For brush-type rubs, however, they would most likely roll in the same direction as the shaft speed, and this behavior has been explained by Adams [18] as inertia-modulated rub which produces a maximum contact force (causing hot spot) 180-degree out of phase with the displacement vibration vector (high spot). Varying 1X vectors can be seen from either proximity probes or casing-mounted transducers.

Bode plots, used to document the change of synchronously filtered amplitude and phase as a function of shaft speed, can be best employed to observe changes in 1X vibration between startup and shutdown conditions. If thermal bow develops as a result of rub prior to shutdown, 1X vibration would be significantly higher during shutdown than during startup, especially near critical speeds. From proximity probes, higher 1X amplitudes can often be observed at very low speed during shutdown due to thermal bow caused by rubs. 1X peak speeds may shift, depending on rub and thermal bow conditions if measured by proximity probes.

Orbit plots, used to display shaft dynamic trajectories from X-Y orthogonally mounted proximity probes, can be employed effectively to identify hard rubs. When these plots are used, they might be compensated by waveform at a low speed to get rid of runout effects and thus to reflect true dynamic motion. Note that this practice of waveform compensation is only applied manually to machinery diagnostics, not treated as a general rule for a permanently installed protection and condition monitoring system. Distorted orbits with abrupt changes usually pinpoint a hard rub. However, it should be noted that a light or mild rub may correspond to seemingly normal orbits. Precession of orbits typically still remains forward.

Waterfall plots, used to track changes in spectral content over a period of time, can be used to observe onset of super-harmonic components above 2X. If vibration is measured by a pair of X-Y orthogonally mounted proximity probes, a full-spectrum waterfall plot is preferred. Distorted orbits due to rub would typically produce super-harmonic components. Since mechanical and electrical runout on the probe-viewing area can also produce rich super-harmonic components, the super-harmonic components due to rub may not be easily identified. Note that a waterfall plot actually derives from orbit/timebase plots. Examining waveform-compensated orbits may be more helpful, unless for cases with a single proximity probe. Casing-mounted transducers can pick up onset of true super-harmonic components due to a rub. Note that a waterfall plot instead of a spectrum plot should be viewed for comparison. A light or mild rub may not be associated with super-harmonic components.

Table 1 – Selection of vibration data plots and key features related to rubs

| Types of plot | Speed conditions | Key features to look for |
|---------------|------------------|---|
| Trend | Steady-state | Varying 1X amplitudes and phase angles; Further review of other plots needed |
| Polar | Steady-state | Varying 1X vectors with reverse rolling or moving radially outward for most rubs, and forward rolling for brush-type rubs |
| Bode | Transient | Significantly higher 1X amplitudes during shutdown than during startup, especially close to critical speeds; higher 1X amplitudes even at low speed and peak response dependent on rub and thermal bow conditions from proximity probes |
| Orbit | All | Distorted orbits (waveform-compensated) with abrupt changes for hard rubs; Smooth orbits possible for mild rubs |
| Waterfall | All | Onset of super-harmonic components above 2X; More reliable with casing transducers than proximity probes due to runout issues; Spectral results of distorted orbits for hard rubs, if measured by proximity probes |

Many rub cases do not lead to opening of machines for inspection and reinstallation of seals or packings. Sometimes rubs can be alleviated by reducing MW to bring vibration levels down, and after experiencing several rubs seal clearance would fit without experiencing further rubs. This could happen on new machines or machines just experiencing an outage. In some cases, rubs are related to process or operation conditions that cause thermal distortion of the machine case, and close monitoring of vibration is needed during that time. Sometimes, seal surface can be contaminated with oil deposits that become carbonized and coked due to high temperature, thus causing rubbing. Identifying rub root-cause and knowing how to control it are imperative to ensure safe operation of the machine.

Conclusions

Based on many rub cases including the three cases demonstrated in this paper, the following conclusions are stated regarding rub diagnostics based on vibration data:

1. Rubs, causing 1X vibration excursions, can be diagnosed successfully by a comprehensive review of vibration data plots. Note that many other malfunctions can also cause 1X vibration excursions.
2. Selection of proper data plots for review and capture of key features to rubs are crucial to the success of rub diagnostics. These plots include trend, polar, Bode, orbit, and waterfall plots.
3. X-Y orthogonally mounted proximity probes are preferred to casing-mounted velocity transducers for capturing not only orbits but also possible shaft thermal bow due to a rub at low speeds.
4. In steady-state or constant speed condition, polar plots are the most important ones for review. Most rubs are accompanied by 1X reverse rolling or radially outward moving vectors while brush-type rubs are often associated with forward 1X rolling vectors.
5. In transient or varying speed condition, Bode plots are the most important ones for review. When a rub and resulting thermal bow exist, 1X vibration versus speed will change its pattern, and during shutdown its amplitude will be significantly higher at critical and low speeds.

References

1. Taylor, H.D., 1924, "Rubbing Shafts Above and Below the resonance Speed," General Electric Company, R-16709, Schenectady, NY.
2. Newkirk, B.L., 1926, "Shaft Rubbing: Relative Freedom of Rotor Shafts from Sensitiveness to Rubbing Contact When Running above Their Critical Speeds," *Mechanical Engineering*, 48 (8), pp. 830-832.
3. Black, H. F. 1967, "Synchronous Whirling of a Shaft Within a Radially Flexible Annulus Having Small Radial Clearance," *IMEchE Paper No. 4*, 18 (65), pp. 29-37.
4. Black, H., 1968, "Interaction of a Whirling Rotor With a Vibrating Stator Across a Clearance Annulus," *J. Mech. Eng. Sci.*, 10(1), pp. 1-12.
5. Crandall, S., 1990, "From Whirl to Whip in Rotordynamics," *IFTOMM 3rd Int. Conf. on Rotordynamics*, Lyon, France, pp. 19-26.
6. Crandall, S. H., and Lingener, A., 1990, "Backward Whirl Due to Rotor-Stator Contact," *Proc. of XII Intl. Conf. Nonlinear Oscillations*, Sept. 2-7, Krakow.
7. Muszynska, A., 1984, "Rotor/Seal Full Annular Rub," *Senior Mechanical Engineering Seminar*, Bently Nevada Corp., Carson City, NV.
8. [Yu, J. J., Goldman, P., Bently, D.E., and Muszynska A., 2002, "Rotor/Seal Experimental and Analytical Study on Full Annular Rub," *ASME J. Eng. Gas Turbines Power*, 124, pp.340-350.
9. Yu, J. J., 2012, "On Occurrence of Reverse Full Annular Rub," *ASME J. Eng. Gas Turbines Power*, 134 (1), p. 012505.
10. Childs, D. W., and Bhattacharya, A., 2007, "Prediction of Dry-Friction Whirl and Whip Between a Rotor and a Stator," *ASME J. Vibr. Acoust.*, 129, pp.355-362.
11. Childs, D. W., and Kumar, D., 2012, "Dry-Friction Whip and Whirl Prediction for a Rotor-Stator Model with Rubbing Contact at Two Locations," *ASME J. Eng. Gas Turbines Power*, 134 (7), p. 072502.
12. Bently, D. E., 1974, "Forced Subrotative Speed Dynamic Action of Rotating Machinery," *ASME Paper No. 74-PET-16*.
13. Yu, J. J., 2010, "Onset of $\frac{1}{2}X$ Vibration and Its Prevention," *ASME J. Eng. Gas Turbines Power*, Vol. 132 (2), p. 022502.
14. Dimarogonas, A.D., 1974, "A Study of the Newkirk effect in Turbomachinery," *Wear*, 28, pp. 369-382.
15. Muszynska, A., 1993, "Thermal Rub Effect in Rotating Machines," *ORBIT*, Bently Nevada Publication, 14 (1), pp. 8-13.
16. Sawicki, J., Montilla-Bravo, A., and Gosiewski, Z., 2003, "Thermomechanical Behavior of Rotor with Rubbing," *Int. J. Rotating Machinery*, 9 (1) pp. 41-47.
17. Keogh, P.S., and Morten, P.G., 1994, "Dynamic nature of Rotor Thermal Bending Due to Unsteady Lubrication Shearing Within a Bearing," *Proc. of Royal Soc., London, Series A: Math. Phys. Sci.*, 445, pp. 273-290.
18. Adams, M.L., 2001, *Rotating Machinery Vibration: From Analysis to Troubleshooting*, Marcel Dekker, New York.



John J. Yu, Ph.D.

Global Technical Leader
Machinery Diagnostic Services
Bently Nevada, a Baker Hughes company

E john.yu@bakerhughes.com